Received: 28 June 2019 | Revised: 28 June 2019 | Accepted: 11 July 2019

DOI: 10.1111/ijac.13332

SPECIAL ISSUE ARTICLE

International Journal of Applied Ceramic TECHNOLOGY

Dense glass-ceramics by fast sinter-crystallization of mixtures of waste-derived glasses

Patricia Rabelo Monich[1] | **Daniel Vollprecht**[2] | **Enrico Bernardo**[1]

[1]Dipartimento di Ingegneria Industriale, Università degli Studi di Padova, Padova, Italy

[2]Chair of Waste Processing Technology and Waste Management, Montanuniversität Leoben, Leoben, Austria

Correspondence
Enrico Bernardo, Dipartimento di Ingegneria Industriale, Università degli Studi di Padova, 35131 Padova, Italy.
Email: enrico.bernardo@unipd.it

Funding information
H2020 Marie Skłodowska-Curie Actions, Grant/Award Number: 721185

Abstract

Dense glass-ceramics were obtained by cold pressing and sinter-crystallization of a glass originated from the plasma gasification of municipal solid waste ("Plasmastone") mixed with recycled soda-lime glass and kaolin clay. The optimum mixture featured 45% Plasmastone/45% soda-lime glass/10% kaolin clay and it was sintered according to a fast heat treatment (30 minutes at 1000°C with heating and cooling rates of approximately 40°C/min), mimicking that of industrial ceramic tiles. The fast treatment avoided extensive crystallization during heating, promoting the viscous flow. In this way, dense glass-ceramics with a water absorption below 0.7% could be produced. The developed tiles presented mechanical properties comparable to those of commercial ceramic tiles. Finally, the environmental impact assessment performed on these materials showed that the leaching of hazardous elements was particularly limited. Microprobe analyses indicated that heavy metals were incorporated in newly formed crystals, consisting mainly of hedenbergite, wollastonite, and iron oxide-rich "islands" surrounded by residual glass. The results show that Plasmastone, combined with recycled soda-lime glass and kaolin clay, may be converted in building materials, with a possible commercial exploitation.

KEYWORDS

crystallization, glass-ceramics, sinter, sintering, crystals

1 | INTRODUCTION

Landfilling is still extensively used as a low-cost way for waste management, despite serious problems that it may cause to the environment and society.[1] For existing landfills, enhanced landfill mining (ELFM) can be an interesting option for remediation strategies.[2] Moreover, ELFM could be also a solution for current issues related to energy production and limited availability of raw materials.[2] Ex-situ ELFM refers to landfill excavation and efficient resource recovery from the excavated waste. After the recovery of part of metals, the excavated waste could be further employed as a solid recovered fuel (SRF) to produce energy by clean technologies such as plasma gasification.[2,3]

In plasma gasification, the organic fraction of the SRF is converted into a synthetic gas ("Syngas"), which can then be upgraded to hydrogen.[3] During this process, the metallic fraction of the SRF can be recovered, while the non-metallic inorganic fraction is vitrified by fast cooling.[3] The obtained vitrified residue ("Plasmastone") can be further upcycled into building materials, such as inorganic polymer binders[3] and porous materials.[4,5] The upcycling of Plasmastone avoids its landfilling and also has the potential to increase the economical profitability of ELFM projects.[2,3]

According to the composition of the SRF and also to the conditions applied in the plasma gasificator, Plasmastone may contain a high quantity of iron oxide.[3] Iron oxides are known to present high solubility in molten glasses, which decreases once the temperature is lowered. By quenching the iron-rich silicate melt, iron oxides remain dissolved in the glass. However, a secondary heating of this iron-rich glass can lead to the separation of the iron oxides, promoting crystallization.[6,7] In fact, previous studies[4,5] have shown that the crystallization tendency of Plasmastone was too high that viscous flow was hindered. This was be easily corrected "a posteriori" by adding up to 30 wt% of soda-lime glass or boro-alumino-silicate glass for porous glass-ceramics.[4,5]

In this study, Plasmastone was once again upcycled into glass-ceramics in order to extend the types of products that could be developed with this vitrified residue, such as tiles. The dense glass-ceramics were produced by cold pressing and sinter-crystallization of Plasmastone mixed with different contents of recycled soda-lime glass. In certain cases, kaolin clay was also added as a binder. Based on the results of water absorption (which is related to the amount of residual open porosity) and density of the samples, several optimizations regarding the composition and the heating treatment were performed. These optimizations were done in order to improve the properties of the glass-ceramic and to employ an approach more compatible to the ceramic industry. The optimized glass-ceramic was finally characterized by means of mechanical tests, environmental impact assessment and physical and morphological analyses. Further characterizations were also done in tiles fired at lower temperature, as a previous study has shown that firing Plasmastone at lower temperature maximized the precipitation of magnetite.[5] Magnetite could in turn bring novel functionalities to the material.[7]

2 | EXPERIMENTAL PROCEDURE

Plasmastone was gently provided by Scanarc (Sweden). The production of this glass is described by Machiels et al.[3] Plasmastone was dried overnight at 100°C and milled until particle size was below 75 μm. Soda-lime glass (mean particle size of 30 μm) was gently provided by company SASIL SpA (Biella, Italy). This fine powder corresponds to the residual waste glass fraction obtained after color selection and separation of polymeric and metallic residues. This glass is not frequently used due to ceramic contaminations.[8] The chemical composition of Plasmastone is reported in Table 1.[4] Moreover, this residue also contained metals like Cu (7124 ppm), Cr (406 ppm), and Ni (203 ppm) which are above the Austrian limit values for recycled building materials.[9] Table 1 also shows the chemical composition of soda-lime glass.[8]

TABLE 1 Chemical composition of Plasmastone and soda-lime glass (wt%)

	Plasmastone	Soda-lime glass
SiO_2	34.26-37.32	71.9
CaO	22.97-23.20	7.5
Fe_2O_3	20.92-24.84	0.3
Al_2O_3	12.82-14.79	1.2
Na_2O	0.26-1.10	14.3
TiO_2	0.60-0.67	0.1
K_2O	0.32-0.51	0.4
MgO	1.18-2.40	4

Differential thermal analysis and thermogravimetric analysis (DTA/TGA, STA409, Netzsch Gerätebau GmbH), were performed on Plasmastone as received (medium particle size of around 10 mm) and on fine powders of this glass (particle size smaller than 75 μm). The heating rate applied was of 10°C/min and the analysis was performed on air.

Dense Plasmastone-derived glass-ceramics were obtained by uniaxially pressing at 50 MPa fine powders of Plasmastone mixed with soda-lime glass (0, 10, 20, or 50 wt%) in a steel die of circular section (diameter of 10 mm) or of squared section (50 mm × 50 mm). The green samples were sintered at 800°C, 900°C, or 1000°C, with different heating rates (10°C/min or 40°C/min), different holding times (30 or 60 minutes), and different cooling rates (normal cooling of the furnace or fast cooling induced by opening the furnace door after the heat treatment was completed). In addition, samples made with a fine mixture of powders of 45 wt% Plasmastone/45 wt% soda-lime glass /10 wt% white kaolin clay were also produced. Kaolin clay was firstly mixed with distilled water (40 wt% of the total solid content) using a mechanical stirrer at 400 rpm. Thereafter, Plasmastone and soda-lime glass were added to the suspension, which was then mixed for 30 minutes and dried overnight at 75°C. After drying, the material was milled with an agate mortar and sieved below 125 μm. The fine powder mixture was pressed at 50 MPa and dried overnight at 75°C before firing.

The water absorption and the density of the sintered discs were measured according to the boiling and Archimedes method, respectively.

The mineralogical composition of fine powders of Plasmastone and Plasmastone-based glass-ceramics was studied by means of X-Ray diffraction (XRD) (Bruker D8 Advance, Germany). Measurements were performed using CuKα radiation (wavelength = 0.15418 nm) in the following operating conditions: 40 kV-40 mA, $2\theta = 15°$-60°, step size 0.05°, 2 seconds counting time. The identification was conducted by means of the Match!® program package (Crystal Impact GbR, Bonn, Germany), supported by data from Powder Diffraction File (PDF)-2 database (International

Centre for Diffraction Data, Newtown Square, PA, USA). For the glass-ceramics, only samples fired following a heating rate of 10°C/min and a holding time of 60 minutes were analysed.

The mechanical properties of the glass-ceramics were assessed by first cutting the fired tiles and polishing the obtained beams up to 5 μm finish using diamond tools. The edges of the beams were carefully polished to remove surface defects. The polished samples presented approximately the following dimensions: 34.3-48.0 mm × 3.4-5.3 mm × 2.6-3.9 mm. Dynamic elastic modulus was measured by nondestructive dynamic resonance and Vickers microhardness was assessed by applying a load of 9.8 N. The four-point bending test (32 mm outer span, 8 mm inner span) was performed using an Instron 1121 UTS instrument (Instron, Danvers, MA) on at least nine specimens with cross-head speed of 1 mm/min. Weibull statistics was applied according to Barsoum,[10] as follow: first, the strength data obtained from bending test were ordered and associated, one by one, to survival probability equal to $P_{s,j} = [(j - 0.3)/(N + 0.4)]$, where j is the number of the sample and N is the total number of samples. Then, the Weibull modulus (m) and the characteristic strength (σ_0^{4pt}) were found by linear regression of strength and probability data in a $\ln[\ln(1/P_s)]/\ln \sigma$ graph)[10] In addition, it was possible to estimate the equivalent strength for three-point configuration using scaling equations based on Weibull modulus and in the hypothesis of flaws occurring with a volume (V_f) or surface (S_f) distribution.[11]

The morphological structure dense Plasmastone-derived glass-ceramics was assessed by scanning electron microscopy (FEI Quanta 200 ESEM, Eindhoven, The Netherlands).

Coefficient of thermal expansion and also porosity of the beams were measured. The porosity was assessed using the software ImageJ on micrographs obtained by scanning electron microscopy.

Leaching tests were done according to the EN 12457-4 with a liquid to solid ratio of 10.[12] This test was performed on the dense sample made with 45 wt% Plasmastone/45 wt% soda-lime glass/10 wt% kaolin clay sintered at 1000°C for 30 minutes according to a fast heating and cooling treatment (named optimized sample). In addition, a commercial tile of "*Ceramiche di Sassuolo*" (Group B II b) was also tested as a control for legal recycling: according to the Austrian Waste Management regulation of 2002, it must be proven that the environmental impact of the recycled product is not worse than that of a competing product from primary raw materials. The dense materials were firstly crushed and sieved below 10 mm. Thereafter, 10 g of each sample was added to an individual bottle containing 0.1 L of distilled water. After 24 hours of mixing by an overhead shaker, the suspension was introduced to a smaller bottle and centrifuged. The heavy metals in the leachate were the measured by inductively coupled plasma mass spectrometry (ICP-MS) and ion chromatography (IC) and compared with the limits allowed by the Austrian Recycling Building Materials Ordinance.[9] Finally, the optimized sample was polished using 1 μm-sized diamond suspension and diamond spray and coated with a fine layer of carbon to be analysed at the microprobe (Jeol JXA 8200 Superprobe). This analysis was performed in order to measure the distribution of main and trace elements and correlate the leaching of heavy metals with the mineralogical phases precipitated.

3 | RESULTS AND DISCUSSION

The DTA (Figure 1) performed on fine and coarse Plasmastone powder shows that the first crystallization peak (T_c) shifted to lower temperatures with particle size reduction. This indicates that this vitrified residue is sensitive to surface crystallization.[13] Figure 1 also shows that fine Plasmastone powder presents three crystallizations peaks: T_c at 800°C, and also two other crystallization peaks around 900°C and 1050°C. These findings were used as a reference for the sintering experiments. Furthermore, the glass transition temperature (T_g) of fine Plasmastone is around 625°C, which is quite close to T_c. This illustrates the high crystallization tendency of Plasmastone upon heating,[14] which may hinder sintering by viscous flow.[13]

According to Machiels et al,[3] Plasmastone was produced under a CO/CO_2 gas mixtures in order to guarantee that Fe is mainly present as Fe^{2+}. Once Plasmastone is heated, Fe^{2+} is oxidized into Fe^{3+},[14,15] which causes a weight gain of around 1.5 wt% after 530°C (Figure 1, TGA plot only for fine powders). In addition, this effect was increased by the high surface-to-volume ratio of the fine powder.[15]

The development of dense Plasmastone-derived glass-ceramics was firstly based on the influence of the heating treatment and addition of soda-lime glass on the density and water

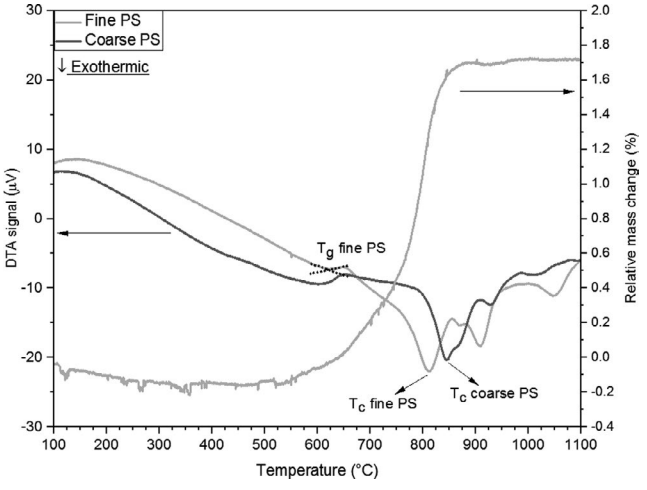

FIGURE 1 DTA and TGA plots for Plasmastone (PS)

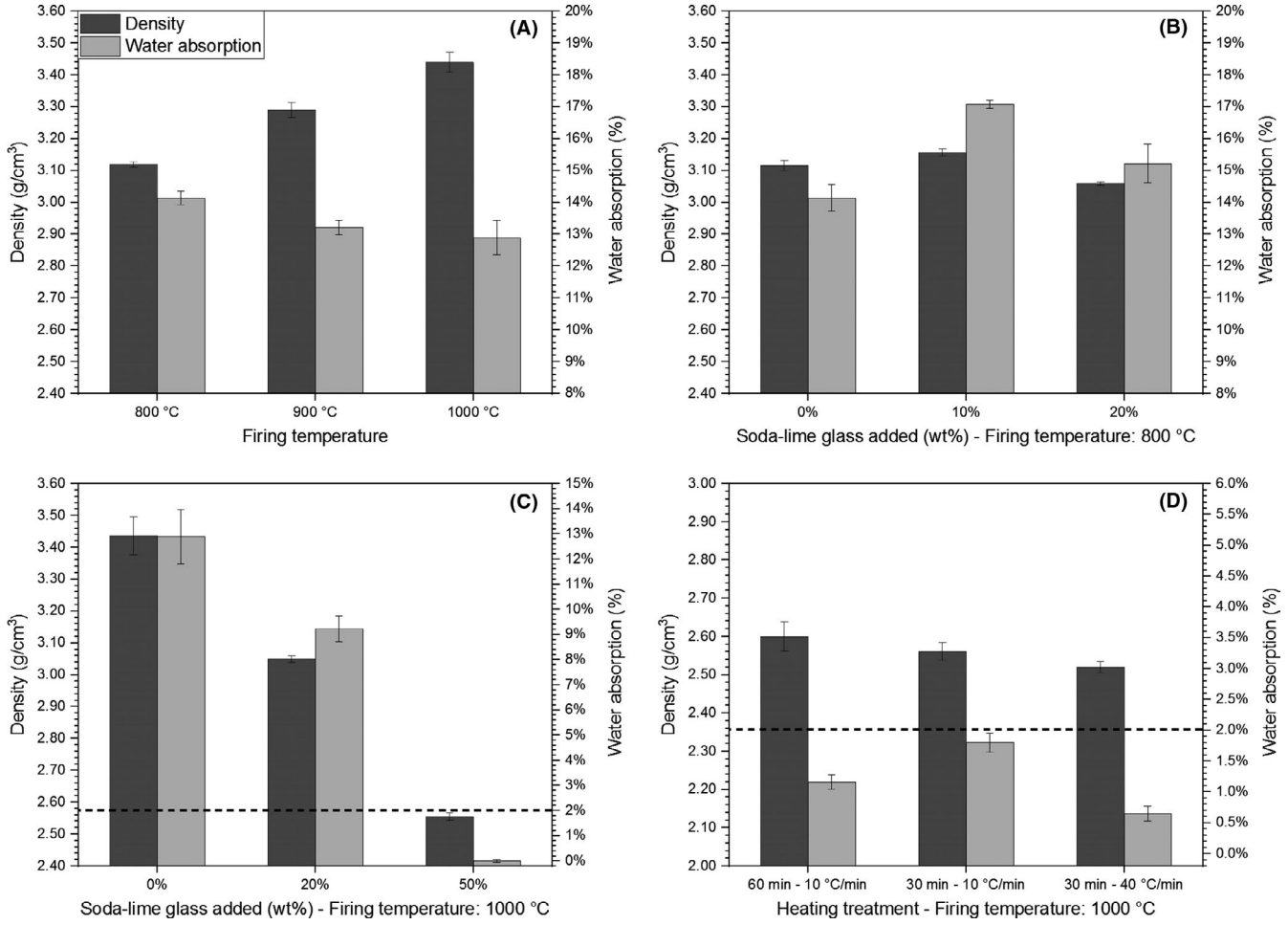

FIGURE 2 Water absorption and density measurements: (A) Plasmastone fired at different temperatures; (B) Plasmastone fired at 800°C with different contents of soda-lime glass; (C) Plasmastone fired at 1000°C with different contents of soda-lime glass; (D) samples from the optimal composition fired at 1000°C with different heating treatments

absorption of the dense materials (Figure 2). First, for pure Plasmastone materials (Figure 2A), the increase in firing temperature indicates a slight improvement in densification: by increasing the firing temperature from 800°C to 1000°C, the density could be increased just by 10%. However, the water absorption for the sample fired at 1000°C (12.89 %) is still too high for products that could replace traditional tiles (the value should be below 2%, for optimized frost resistance).[13] In this case, the increase in viscosity due to the precipitation of crystals hindered viscous flow, thus affecting the densification of the material, as previously mentioned.[4] In addition, the oxidation of Fe^{2+} (as indicated by the TGA of Figure 1), may increase the viscosity of the liquid glass phase, thus affecting the densification of Plasmastone.[16,17]

Based on these results, recycled soda-lime glass was introduced to promote viscous flow.[4,18] Samples made with different contents of soda-lime glass were fired at 800°C or 1000°C, that is, at the two "end temperatures" previously tested for pure Plasmastone. Figure 2B,C show that, quite surprisingly, the water absorption did not increase significantly at 800°C, for all contents, whereas some changes were observed at 1000°C. Samples with nearly zero water absorption could be finally developed with 50 wt% soda-lime glass; in this case, however, there was also a decrease in density. This could be firstly attributed to simple density variations in the constituents (soda-lime glass is lighter than Plasmastone: 2.5 g/cm^3 against 3.1 g/cm^3). Second, we cannot exclude a contribution from bloating: at higher temperatures, Fe^{3+} can be partially reduced to Fe^{2+}, releasing oxygen which may remain trapped inside the viscous mass, causing a decrease in density.[19] This phenomenon may have been more pronounced for mixtures of 50 wt% Plasmastone/50 wt% soda-lime glass fired at 1000°C, as the quantity of glass phase was greater and less viscous, thus increasing the medium available for foaming.[20]

After selecting the optimal quantity of soda-lime glass, 10 wt% kaolin clay was also introduced as a binder to improve the pressing step and reduce demoulding flaws.[8] In this case, the water absorption increased to 1.16%. As the value is still below the threshold for ceramic tiles, the composition of 45%

Plasmastone/45% soda-lime glass/10% kaolin clay was selected as the optimal one. Thereafter, other optimizations (Figure 2D) were performed in order to improve the thermal treatment and mimic as much as possible the one applied by the ceramic industry. First, the holding time was reduced from 60 to 30 minutes, which caused an increase in the water absorption to 1.80%. Thereafter, the heating and cooling rates were increased in order to simulate industrial production.[8] Aside from being more economical, the fast heating treatment decreased the water absorption to 0.65%. Previous studies[21–23] have shown that higher heating rates prevent extensive crystallization upon heating. In this way, viscous flow is promoted, decreasing the water absorption of the sample. Therefore, the group of samples 45% Plasmastone/45% soda-lime glass/10% kaolin clay fired up to 1000°C with a fast heating and cooling rate was considered the optimal one and used for most of the following characterizations.

The X-ray diffraction patterns in Figure 3 evidence the microstructural evolutions taking place upon firing. Starting with pure Plasmastone (Figure 3A), it can be observed that the as received material presents the characteristic amorphous "halo" of glasses. Once this residue is fired, Plasmastone is prone to crystallization, as indicated by Figure 2A. For samples fired at 800°C, the main signals are mainly consistent to those of Ca-Fe rich pyroxene (hedenbergite, $Ca(Fe_{0.821}Al_{0.179})(SiAl_{0.822}Fe_{0.178}O_6)$, PDF no. 78-1546). For temperatures above 900°C, andradite ($Ca_3Fe_2(SiO_4)_3$, PDF#84-1935) can also be detected. This indicates that the first crystallization peak in Figure 1 likely refers to the crystallization of pyroxenes while the second peak (at around 900°C) refers to andradite.

For samples fired at 800°C (Figure 3B), the addition of soda-lime glass promoted the precipitation of wollastonite ($CaSiO_3$, PDF no. 84-0655). In contrast with what observed for Plasmastone/soda-lime glass foams fired at 1000°C,[4] the addition of soda-lime glass promoted the formation of pyroxenes for firing at 800°C. A possible explanation for this could be that soda-lime glass helped to decrease the apparent activation energy for crystal growth due to an increase in the alkali content, promoting crystallization.[24] In addition, many peaks of the Ca-Fe silicates phases (Figure 3A,B) overlapped with those of hematite "H" (Fe_2O_3, PDF no. 89-2810) and magnetite "M" (Fe_3O_4, PDF no. 89-0691). The presence of magnetite, for samples fired at 800°C (Figure 3B), is most probable since they were attracted by a permanent magnet.[4]

In contrast to Figure 3B, the introduction of 50 wt% soda-lime glass decreased the crystallization of Ca–Fe silicates for samples fired at 1000°C (Figure 3C). In fact, signals consistent to those of andradite are extremely weak for samples made with soda-lime glass. Regarding the samples made with the optimal composition (45% Plasmastone/45% soda-lime glass/10% kaolin clay) fired at 1000°C, quartz (SiO_2, PDF no. 83-0539) and cristobalite (SiO_2 PDF no. 89-3607) were also detected, due to contaminations of kaolin clay.

Table 2 shows the mechanical properties of the optimized sample and also of dense materials fired at a lower

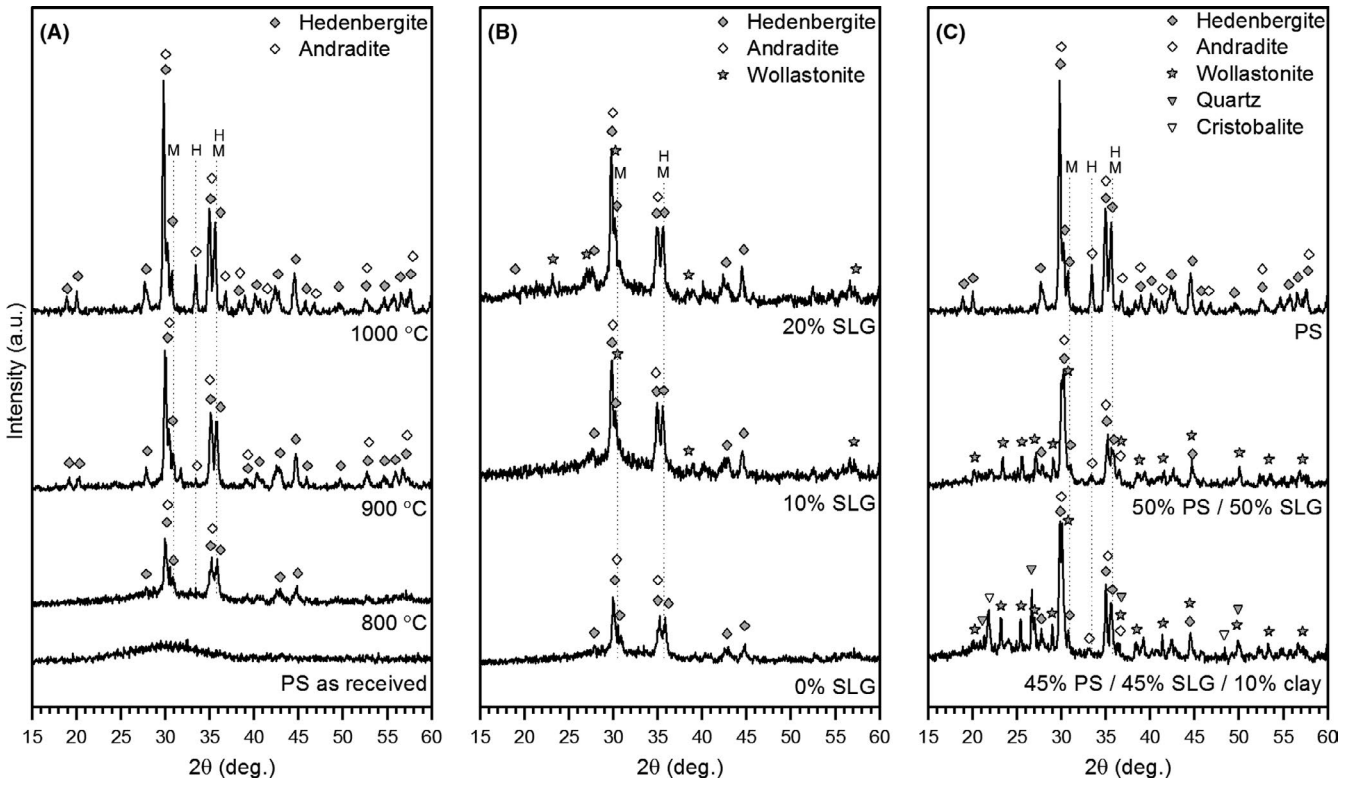

FIGURE 3 Mineralogical characterization of Plasmastone-derived materials: (A) Pure Plasmastone fired at 800°C, 900°C or 1000°C; (B) Plasmastone-based glass-ceramics fired at 800°C; (C) Plasmastone-based glass-ceramics fired at 1000°C

TABLE 2 Physical and mechanical properties of Plasmastone-derived glass-ceramics

Sample	Elastic modulus (GPa)	*M*	Strength (MPa)		
			σ_0^{4pt}	σ_{eq}^{3pt}	σ_{eq}^{L}
Optimized sample	76.8 ± 2.5	10.9	69.83	76.6^{Vf}	39.3^{Vf}
				76.4^{Sf}	43.1^{Sf}
80% Plasmastone/20% soda-lime glass—800°C	48.5 ± 4.5	7.4	20.05	22.8^{Vf}	8.6^{Vf}
				22.6^{Sf}	9.8^{Sf}
90% Plasmastone/10% soda-lime glass—800°C	38.9 ± 2.5	4.7	13.07	15.6^{Vf}	3.3^{Vf}
				15.1^{Sf}	4.0^{Sf}

M, Weibull modulus; σ_0^{4pt}, characteristic strength; σ_{eq}^{3pt}, equivalent strength in a three-point configuration with cross-section of 3 mm × 4 mm (loading span of 40 mm); σ_{eq}^{L}, equivalent strength for tiles with cross-section of 8 mm × 300 mm (loading span of 300 mm); Vf, flaws hypothetically occurring with a volume distribution; Sf, flaws hypothetically occurring with a surface distribution

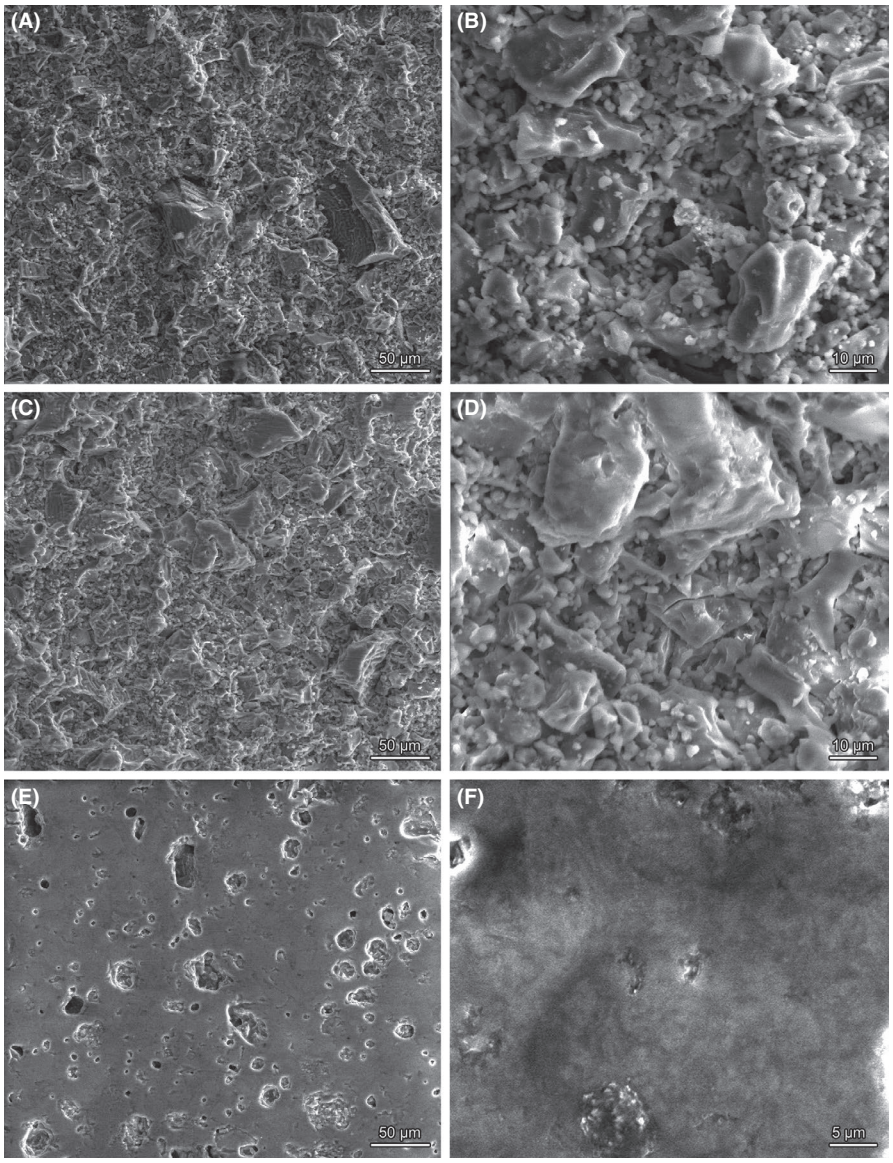

FIGURE 4 Micrographs of Plasmastone-derived glass-ceramics. (A-B) 90% Plasmastone/10% soda-lime glass fired at 800°C; (C-D) 80% Plasmastone/20% soda-lime glass fired at 800°C; (E-F) optimized sample

temperature with less soda-lime glass. The optimized sample presents properties similar to other commercial tiles: the elastic modulus is comparable to the one of a commercial porcelain stoneware.[25] The scaling of strength estimated that the equivalent strength σ_{eq}^{3pt} in a three-point configuration of the optimized sample with standard

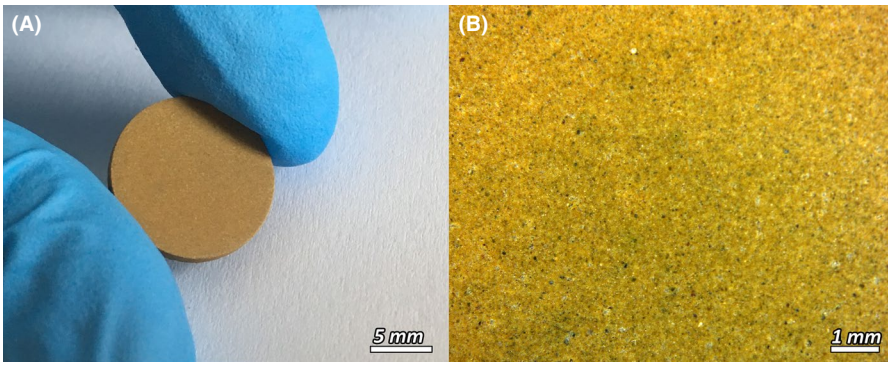

FIGURE 5 (A) Esthetic appearance of optimized glass-ceramic sample; (B) optical micrograph (real colors) [Color figure can be viewed at wileyonlinelibrary.com]

TABLE 3 Results of the leaching test of the control and optimized samples (mg/kg DM)

	U-A	U-B	D	Control	Optimised Sample
Cr	0.6	1.0	0.3	0.017	0.088
Cu	1.0	2.0		0.19	0.33
Ni	0.4	0.6		0.042	0.019
Cl	800	1000		5.9	3.4
SO_4	2500	6000		19	32
Ba			20	0.029	0.13
Cd			0.04	0.001	0.0015
Co			1	2.9	0.018
Mo			0.5	0.12	1.5
Tl			0.1	<0.0010	0.0041
V			1	0.26	0.064
W			1.5	2.8	0.18
F			10	4.2	2.6

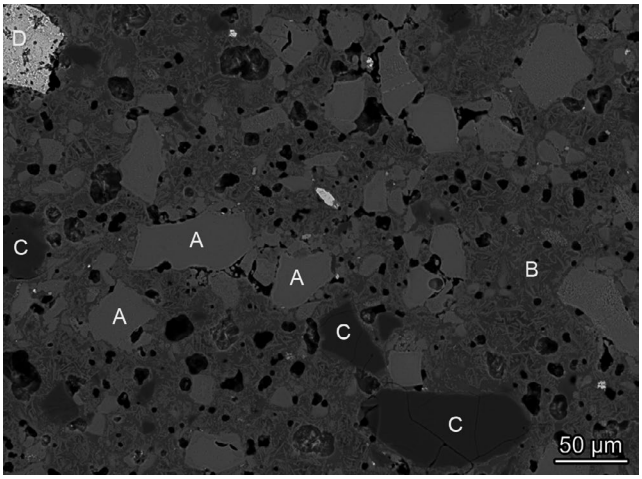

FIGURE 6 Micrograph of the optimized sample: (A) hedenbergite; (B) glass/wollastonite zone; (C) silica; (D) iron oxide

geometry (cross-section of 3 mm × 4 mm and loading span of 40 mm) is 76 MPa. Moreover, the equivalent strength for bigger tiles σ_{eq}^{L} (cross-section of 8 mm × 300 mm and loading span of 300 mm) is above the lower strength limit (35 MPa) for the best materials to be applied as tiles (BI_a group).[26] Regarding the materials fired at 800°C with up to 20 wt% soda-lime glass, the mechanical properties were much lower. However, in any case, the properties compare well with the reference minimum value (15 MPa, for bending strength of tiles with thickness below 7.5 mm) for highly porous tiles (BIII group).[26] The presence of magnetite (enhanced for the sample sintered at 800°C with an addition of 20% soda-lime glass—see Figure 3B) could be also exploited for some electromagnetic shielding, in analogy with what found in the recent literature.[5,27]

The micrographs of Plasmastone-derived glass-ceramics fired at lower temperature (Figure 4A-D) explain their low mechanical performance: it can be seen that these groups of samples were poorly densified, as already indicated by the water absorption results (Figure 2B). In contrast to these samples, the optimized sample (Figure 4E,F) was well densified by viscous flow, with an estimated porosity equal to 5%. In addition, the presence of coarse pores indicates that the bloating phenomenon took place upon heating,[19] as previously mentioned.

As the optimized sample showed the best results so far, this group of samples was selected for further characterizations. The measured microhardness of this material was of 5.3 ± 0.04 GPa, which is a similar value of other waste-derived glass-ceramics.[20,28] In addition, the coefficient of thermal expansion ($9.5 \times 10^{-6}°C^{-1}$), is also comparable to the ones already measured in waste-derived glass-ceramic materials.[28] Figure 5A shows the typical appearance of optimized sample, exhibiting a brown-bronze coloration. The good densification is further testified by the optical micrograph in Figure 5B.

In order to safely apply waste-derived materials, the chemical stability of the developed material must be assessed through leaching tests. In this study, the leaching test (Table 3) was performed in the optimized sample and in a commercial tile applied as a control. On the one hand, the results show that the optimized sample is within the Austrian regulation for classes U-A and U-B (quality classes for recycled construction materials used in unbound or (hydraulically/bituminously) bound applications

TABLE 4 Results of the microprobe analysis

Phase	Mo (%)	Fe (%)	Cu (%)	Ba (%)	Zn (%)	V (%)	Cr (%)
a) Hedenbergite	0.01	13.3	0.20	0.03	0.06	0.04	0.13
b) Residual glass/wollastonite zone	0.03	3.50	0.25	0.03	0.05	0.01	0.03
c) Silica	0.01	0.18	0.01	0.00	0.00	0.00	0.00
d) Iron Oxide	0.00	62.1	0.41	0.00	0.03	0.02	0.10

as aggregate) with respect to leachability, even if the total contents of Cu, Cr, and Ni exceeded the Austrian limit values for recycled building materials. On the other hand, the high quantity of Mo leached prevented the classification of the optimized sample as class D (relevant for slags). However, one must observe that the control sample also presented leaching values of certain metals (Co and W) above the ones accepted for Class D.

The micrograph of the optimized sample (Figure 6) is consistent to the XRD analysis of the sample 45% Plasmastone/45% soda-lime glass/10% kaolin clay fired at 1000°C (Figure 3C). The crystalline phases are embedded in the glassy phase, which aids in sealing hedenbergite. Moreover, silica (quartz and cristobalite) and iron oxide can be identified, as well as wollastonite, which presents a needle morphology. It was not possible to identify andradite, which is presented in a lower amount in samples made with the optimized composition fired at 1000°C (see Figure 3C). Finally, the porosity is closed and similar to the one of industrial tiles.

Electron microprobe analyses (Table 4) explain the low leaching of heavy metals due to their incorporation in stable mineral phases: Cu is mainly distributed in iron oxide and Cr and V in hedenbergite. This is consistent with the literature on the incorporation of Cu in iron oxides[29] and inclusion of Cr and V in pyroxenes.[30–32] Hedenbergite is also known for its chemical stability.[33] Zn and Ba are evenly bonded among hedenbergite and glass/wollastonite zone (it was not possible to perform the quantitative analysis separately in these phases, due to the insufficient spatial resolution of the microprobe). Mo, which was the only element with a leachable content above the Class D, is mainly distributed in the glass/wollastonite zone. The high leaching of this metal was already observed in porous Plasmastone-derived glass-ceramics: once Plasmastone/soda-lime glass mixtures are fired, wollastonite is formed (as observed in Figure 3C). This increases the alkali content of the residual glass phase and can favor the network dissolution, releasing elements such as Mo.[4,34]

4 | CONCLUSION

We may conclude that:

1. Dense and strong Plasmastone/soda-lime glass/kaolin clay glass-ceramics can be produced by cold-pressing and fast sinter-crystallization.
2. The high amount of iron oxide in Plasmastone is responsible for two effects in the glass-ceramic: firstly, crystallization is promoted thus affecting sintering by viscous flow; Second, bloating can be favored in samples with a higher quantity of glass phase with low viscosity, thus decreasing the density.
3. Sintering by viscous flow is promoted by introducing soda-lime glass and by increasing the sintering temperature and heating rate.
4. The produced glass-ceramics present low water absorption, low leachability, and high mechanical properties when compared with commercial ceramic tiles. This indicates that Plasmastone (when mixed with soda-lime glass and kaolin clay) may be upcycled into tiles, with a possible commercial exploitation.

ACKNOWLEDGMENTS

The research leading to these results has received funding from the European Union's Horizon 2020 research and innovation programme under the Marie Sklodowska-Curie grant agreements No. 721185 “NEW-MINE” (EU Training Network for Resource Recovery through Enhanced Landfill Mining; website: http://new-mine.eu/).

CONFLICT OF INTEREST

None.

ORCID

Patricia Rabelo Monich https://orcid.org/0000-0003-0436-8091

Enrico Bernardo https://orcid.org/0000-0003-4934-4405

REFERENCES

1. Krook J, Svensson N, Eklund M. Landfill mining: a critical review of two decades of research. Waste Manag. 2012;32(3):513–20.

2. Jones PT, Geysen D, Tielemans Y, Van Passel S, Pontikes Y, Blanpain B, et al. Enhanced landfill mining in view of multiple resource recovery: a critical review. J Clean Prod. 2013;55:45–55.
3. Machiels L, Arnout L, Yan P, Jones PT, Blanpain B, Pontikes Y. Transforming enhanced landfill mining derived gasification/vitrification glass into low-carbon inorganic polymer binders and building products. J Sustain Metall. 2017;3(2):405–15.
4. Monich PR, Romero AR, Höllen D, Bernardo E. Porous glass-ceramics from alkali activation and sinter-crystallization of mixtures of waste glass and residues from plasma processing of municipal solid waste. J Clean Prod. 2018;188:871–8.
5. Monich PR, Desideri D, Bernardo E. Low temperature upcycling of vitreous byproduct of the MSW plasma processing into multifunctional porous glass-ceramics. Adv Appl Ceram. 2019;118(6):366–71.
6. Höland W, Beall GH. Glass-ceramic technology. Hoboken, NJ: John Wiley & Sons, Inc.; 2012.
7. Chinnam RK, Francis AA, Will J, Bernardo E, Review B. Functional glasses and glass-ceramics derived from iron rich waste and combination of industrial residues. J Non Cryst Solids. 2013;365(1):63–74.
8. Marangoni M, Ponsot I, Kuusik R, Bernardo E. Strong and chemically inert sinter crystallised glass ceramics based on Estonian oil shale ash. Adv Appl Ceram. 2014;113(2):120–8.
9. RIS - Recycling-Baustoffverordnung (Austrian Recycling Building Materials Ordinance). 2019. https://www.ris.bka.gv.at/GeltendeFassung.wxe?Abfrage=Bundesnormen&Gesetzesnummer=20009212.
10. Barsoum MW. Fundamentals of ceramics. Bristol: Institute of Physics Publications; 2003.
11. Quinn GD. Weibull strength scaling for standardized rectangular flexure specimens. J Am Ceram Soc. 2003;86(3):508–10.
12. BS EN 12457–4:2002. Characterisation of waste. Leaching. Compliance test for leaching of granular waste materials and sludges. 2002.
13. Rincón A, Marangoni M, Cetin S, Bernardo E. Recycling of inorganic waste in monolithic and cellular glass-based materials for structural and functional applications. J Chem Technol Biotechnol. 2016;91(7):1946–61.
14. Karamanov A, Pisciella P, Cantalini C, Pelino M. Influence of Fe^{3+}/Fe^{2+} ratio on the crystallization of iron-rich glasses made with industrial wastes. J Am Ceram Soc. 2000;83(12):3153–7.
15. Marangoni M, Arnout L, Machiels L, Pandelaers L, Bernardo E, Colombo P, et al. Porous, sintered glass-ceramics from inorganic polymers based on fayalite slag. J Am Ceram Soc. 2016;99(6):1985–91.
16. Karamanov A, Taglieri G, Pelino M. Sintering in nitrogen atmosphere of iron-rich glass-ceramics. J Am Ceram Soc. 2004;87(7):1354–7.
17. Karamanov A, Maccarini Schabbach L, Karamanova E, Andreola F, Barbieri L, Ranguelov B, et al. Sinter-crystallization in air and inert atmospheres of a glass from pre-treated municipal solid waste bottom ashes. J Non Cryst Solids. 2014;389:50–9.
18. Bernardo E, Bonomo E, Dattoli A. Optimisation of sintered glass-ceramics from an industrial waste glass. Ceram Int. 2010;36(5):1675–80.
19. Appendino P, Ferraris M, Matekovits I, Salvo M. Production of glass-ceramic bodies from the bottom ashes of municipal solid waste incinerators. J Eur Ceram Soc. 2004;24(5):803–10.
20. Ponsot I, Pontikes Y, Baldi G, Chinnam R, Detsch R, Boccaccini A, et al. Magnetic glass ceramics by sintering of borosilicate glass and inorganic waste. Materials. 2014;7(8):5565–80. https://doi.org/10.3390/ma7085565.
21. Bernardo E. Fast sinter-crystallization of a glass from waste materials. J Non Cryst Solids. 2008;354(29):3486–90.
22. Karamanov A, Pelino M, Hreglich A. Sintered glass-ceramics from Municipal Solid Waste-incinerator fly ashes-part I: the influence of the heating rate on the sinter-crystallisation. J Eur Ceram Soc. 2003;23(6):827–32.
23. Lu J, Lu Z, Peng C, Li X, Jiang H. Influence of particle size on sinterability, crystallisation kinetics and flexural strength of wollastonite glass-ceramics from waste glass and fly ash. Mater Chem Phys. 2014;148(1–2):449–56.
24. Watanabe T, Hashimoto H, Hayashi M, Nagata K. Effect of alkali oxides on crystallization in $CaO–SiO_2–CaF_2$ glasses. ISIJ Int. 2008;48(7):925–33.
25. Buchner S, Mikowski A, Lepienski CM, Ferreira EB, Zanotto ED, Torres RD, et al. Mechanical and tribological properties of a sintered glass-ceramic compared to granite and porcelainized stoneware. Wear. 2011;271(5–6):875–80.
26. BS EN 14411:2016 - Ceramic tiles - Definition, classification, characteristics, assessment and verification of constancy of performance and marking. 2016.
27. Rincón A, Desideri D, Bernardo E. Functional glass-ceramic foams from 'inorganic gel casting' and sintering of glass/slag mixtures. J Clean Prod. 2018;187:250–6.
28. Bernardo E, Dal Maschio R. Glass-ceramics from vitrified sewage sludge pyrolysis residues and recycled glasses. Waste Manag. 2011;31(11):2245–52.
29. Piatak NM, Seal RR. Mineralogy and environmental geochemistry of historical iron slag, Hopewell Furnace National Historic Site, Pennsylvania, USA. Appl Geochemistry. 2012;27(3):623–43.
30. Lottermoser BG. Mobilization of heavy metals from historical smelting slag dumps, north Queensland, Australia. Mineral Mag. 2002;66(4):475–90.
31. Karner JM, Papike JJ, Sutton SR, Shearer CK, Burger P, McKAY G, et al. Valence state partitioning of V between pyroxene-melt: effects of pyroxene and melt composition, and direct determination of V valence states by XANES. Application to Martian basalt QUE 94201 composition. Meteorit Planet Sci. 2008;43(8):1275–85.
32. Simon SB, Sutton SR, Grossman L. Valence of titanium and vanadium in pyroxene in refractory inclusion interiors and rims. Geochim Cosmochim Acta. 2007;71(12):3098–118.
33. Pisciella P, Crisucci S, Karamanov A, Pelino M. Chemical durability of glasses obtained by vitrification of industrial wastes. Waste Manag. 2001;21(1):1–9.
34. Bunker BC. Molecular mechanisms for corrosion of silica and silicate glasses. J Non Cryst Solids. 1994;179:300–8.

How to cite this article: Rabelo Monich P, Vollprecht D, Bernardo E. Dense glass-ceramics by fast sinter-crystallization of mixtures of waste-derived glasses. *Int J Appl Ceram Technol*. 2020;17:55–63. https://doi.org/10.1111/ijac.13332